MATHEMATICAL ENHANCEMENT OF DATA

FROM SCIENTIFIC MEASURING INSTRUMENTS

NASA RESEARCH GRANT NO. NAG 1-16

(NASA-CR-169973) MATHEMATICAL ENHANCEMENT OF DATA FROM SCIENTIFIC MEASURING INSTRUMENTS Final Report, 1 Jul. - 31 Dec. 1982 (Xavier Univ. of Louisiana, New Orleans.) 36 p HC A03/MF A01 CSCL 14B G3/35

N83-19071

Unclas 02930

FINAL REPORT

1 July 1982 to 31 December 1982

Juliette W. Ioup
Principal Investigator
Physics/Pre-Engineering Department
Xavier University
New Orleans, LA 70125
(504) 486-7411 ext 647

MATHEMATICAL ENHANCEMENT OF DATA FROM SCIENTIFIC MEASURING INSTRUMENTS

Introduction

The accuracy of any physical measurement is limited by the instruments performing it. The proposed activities of this grant are related to the study of and application of mathematical techniques of deconvolution. Two techniques are being investigated: an iterative method and a function continuation Fourier method. This final status report describes the work performed during the period July 1 to December 31, 1982.

Discussion

During the academic year 1982-83, the Principal Investigator is on leave from her position as Professor of Physics at Xavier University. Her present position is as a Geophysicist Data Processor processing seismic data for Texaco in New Orleans. Geophysical processing includes deconvolution and therefore is closely related to the goals of this grant. Various schools and short courses have been attended to provide a broader background in geophysics.

The NASA Technical Officer for this grant, Dr. George M.

Wood, Jr., spent the summer in New Orleans working with Dr. George E. Ioup, of the Department of Physics at the University of New Orleans, and with the Principal Investigator. The research performed is described in the paper, "Iterative and Function-Continuation-Fourier Deconvolution Methods for Enhancing Mass Spectrometer Resolution." A copy of the current draft of this paper is attached. It will be submitted for publication in the International Journal of Mass Spectrometry and Ion Physics.

Publication

The abstract of a talk presented at the Louisiana Academy of Sciences, "The Convolution Integral in Geophysics," has appeared in the Proceedings of the Louisiana Academy of Sciences, Vol. XLV, page 193, published in 1982.

ITERATIVE AND FUNCTION-CONTINUATION-FOURIER DECONVOLUTION METHODS FOR ENHANCING MASS SPECTROMETER RESOLUTION*

Juliette W. Ioup, Physics/Pre-Engineering Department, Xavier University, New Orleans, LA 70125, and Texaco,† P.O.Box 60252, New Orleans, LA 70160,

George E. Ioup, Department of Physics, University of New Orleans, New Orleans, LA 70148,

Grayson H. Rayborn, Jr., Department of Physics and Astronomy, University of Southern Mississippi, Hattiesburg, MS 39401,

George M. Wood, Jr., NASA Langley Research Center, Hampton, VA 23665, and

Billy T. Upchurch, Department of Chemistry, Old Dominion University, Norfolk, VA 23508.

Abstract

Mass spectrometer data in the form of ion current versus mass-to-charge ratio often include overlapping mass peaks, especially in low and medium resolution instruments. Numerical deconvolution of such data effectively enhances the resolution by decreasing the overlap of mass peaks. In this paper two approaches to deconvolution are presented: a function domain iterative technique and a Fourier-transform method which uses transform domain function continuation. Both techniques include data smoothing to reduce the sensitivity of the decon-

volution to noise. The efficacy of these methods is demonstrated through application to representative low resolution mass spectrometer data and the deconvolved results are discussed and compared to data obtained from a spectrometer with sufficient resolution to achieve separation of the mass peaks studied.

*Supported in part by NASA Research Grants NAG 1-16 (Xavier University), NSG-1460 and NSG-1648 (University of New Orleans), and NSG-1285 and NSG-1380 (University of Southern Mississippi).

†Present address.

ITERATIVE AND FUNCTION-CONTINUATION-FOURIER DECONVOLUTION METHODS FOR ENHANCING MASS SPECTROMETER RESOLUTION

Introduction

The accuracy of any physical data measurement is limited by the resolving power of the instrument performing the measurement. There exist, however, suitable mathematical techniques which may be applied in order to increase the useful information which may be extracted. Broadening or lack of resolution in the experimental data may be described by the convolution integral if the system is shift invariant, i.e., if the response of the system does not change significantly as the measurements progress. If the response of the system is known, one may go from the detected signal at least partly back to the ideal, or unbroadened, signal by using mathematical techniques of noise removal and deconvolution.

A parallel problem in data collection is that of noise, which is present in all measurements. The adjustment of instrumental parameters to enhance resolution decreases the signal-to-noise ratio, with a resultant loss of sensitivity. The analysis of mass spectrometric data may therefore be facilitated by the use of deconvolution with noise removal features since this

process is able to separate the signal from some of the noise.

Mass spectrometer data in the form of ion intensity versus mass often include overlapping mass peaks, especially in low-to-moderate resolution spectrometers. For such poorly resolved data, the identification of masses and relative abundance measurements can be difficult. Effective increase of the resolution by numerical deconvolution of the data can increase the separation of overlapping peaks and lead to improved analysis.

In this work two approaches to deconvolution are used: a function domain iterative technique and a Fourier method which uses transform domain function continuation. These techniques are briefly discussed in the following sections.

Iterative Method of Deconvolution

Let h represent the observed distribution of data, f the true or ideal distribution, and g the apparatus or instrument response function. These quantities are related by the convolution of f with g:

$$h(x) = \int_{-\infty}^{\infty} f(y)\, g(x-y)\, dy \equiv f * g \qquad (1)$$

Physically this means that the ideal or true data describing the physical process, f, are smeared out or broadened by the measuring apparatus or other experimental features, all represented by a response function, g, to produce the data, h, which are actually observed. The problem is to remove the broadening effects and

obtain the ideal f from the measured h by deconvolution. Mathematically this is described as solving a Fredholm integral equation of the first kind with a difference kernel.

Morrison's iterative noise removal technique first smoothes the data, then iteratively restores the non-noisy output and the compatible noise. It was designed specifically to prepare data for deconvolution. The initial smoothing produces data h_1:

$$h_1 = h * g \quad . \tag{2}$$

The nth restoration is given by

$$h_n = h_{n-1} + (h - h_{n-1}) * g \qquad n \quad 1 \quad . \tag{3}$$

After the data are smoothed and then resotred the selected number of iterations, van Cittert's iterative deconvolution or unfolding method may be applied. The first unfolded f is assumed to be the same as h:

$$f_o = h \quad , \tag{4}$$

while the nth unfolding is given by

$$f_n = f_{n-1} + (h - f_{n-1} * g) \quad . \tag{5}$$

A major difficulty of the iterations is that they do not converge for most response functions. The iterative approach has been modified by one of us so that convergence is achieved.

It is necessary to study the particular data to be treated in order to determine the number of smoothings and the number of unfoldings needed. Convergence checks can be applied to the output of each successive smoothing and unfolding. The usual procedure is to compute several iterations and compare the output from each. In general, for noisier data, after the initial smoothing, fewer restorations and also fewer unfoldings should be used since deconvolution amplifies noise. In mass spectrometer data, the signal-to-noise ratio is affected by the slit widths in the instrument as well as other factors. In any experiment there is typically a trade-off between the instrument resolution and the noise in the data. If the instrument is tuned for more resolution, the signal-to-noise ratio will decrease. When there is more noise present in the data at high resolution, smoothing may be emphasized. When there is less noise present with lower resolution, deconvolution may be emphasized. Judicious application of the mathematical treatment will in either case enhance the information obtained from the raw data.

Function-Continuation-Fourier Method of Deconvolution

The Fourier transform may be used to deconvolve data because the convolution in the function domain,

$$h = f * g \qquad (1)$$

becomes a simple multiplication in the Fourier transform domain

according to the convolution theorem. Let the Fourier transforms be represented by capital letters, i.e., the Fourier transform of f is F, etc.:

$$F(s) = \int_{-\infty}^{\infty} f(x) \exp(-i2\pi xs)\, dx \quad . \tag{6}$$

The inverse Fourier transform is

$$f(x) = \int_{-\infty}^{\infty} F(s) \exp(i2\pi xs)\, ds \quad . \tag{7}$$

The equation in the Fourier domain corresponding to the convolution in the function domain is given by the convolution theorem,

$$H = F\,G \quad . \tag{8}$$

F may be obtained by

$$F = H/G \quad , \tag{9}$$

if G is not zero. The inverse Fourier transform is then computed to obtain f. This procedure is generally called transform domain inverse filtering. Since noise often predominates at high frequencies, the high frequency part of the spectrum is generally deleted (a process called (ideal) low-pass filtering) before inverse filtering.

Because of the noise problem at high frequencies, only the low frequency values are used to calculate a solution f_ℓ in the function continuation Fourier method. Since the higher frequencies are often important for obtaining improved resolution, the result

f_ℓ obtained from the low-pass inverse filtering is enhanced by the technique of function domain fitting. In this procedure an artificial function, a, is constructed by fitting an appropriate function (in this case a Gaussian) to the peaks of the function f_ℓ. The Fourier transform A is obtained, and the Fourier coefficients of A and F are compared. Because of the noise dominance at high frequencies, the high frequency coefficients of F are replaced with the high frequency coefficients of A, which are not affected by noise. The low frequency components of F, which determine the principal features of the devonvolved result, are unchanged.

Recently, Amaya et al applied low-pass inverse filtering to mass analyzed data to remove the parent ion beam spread. They obtained significantly improved resolution, but because they gave up the high frequency information to obtain smoothing and because they were only removing parent ion beam spread, the improvement was not as much as it could have been. Both approaches in this paper include some high frequency information. The iterative deconvolution approach resotres an increasing amount of this information with each iteration. It also uses a function-domain non-negativity constraint to determine the high frequency part of the spectrum. The function-continuation-Fourier method uses an artificial function to restore the high frequencies.

Some other aspects of the procedures of Amaya et al merit discussion. In recording the data, they reduced the size of their

data file by keeping only one in a selected number of points, m, with m determined by the size reduction needed. Such an approach can possibly introduce aliasing error if the data are not first filtered. In order to account for differing mass-to-charge ratios of parent and daughter ions, the main beam peak also had points deleted. To reduce aliasing (referred to as a low frequency pattern by the authors) successive three-point smoothing was used. This smoothing does reduce aliasing, but it may also have an undesirable effect on the deconvolution. The smoothing is equivalent to multiplication by $(\sin \pi ws/\pi ws)^n$ in the transform domain (with s the transform domain variable, n the number of times the smoothing is applied, and w determined by the number of points averaged), and if n is small, large sidelobes are possible in the transform domain which could distort a subsequent deconvolution.

After deconvolving, Amaya et al set negative oscillations to zero. This method of applying constraints after the solution is obtained is not advisable since the result is no longer a solution to the convolution equation, the area relation of the convolution is no longer preserved, and the constraints cannot beneficially affect the rest of the solution. Both the present approaches use the minimization of negative excursions to extend the transform solution to higher frequencies without affecting the low-frequency part of the transform. The iterative procedure strictly conserves area and the Fourier-related method can easily be adjusted to do so. Amaya et al also keep maximum intensities equal before and

after deconvolution. This may not be a desirable procedure since sharpening a peak will cause its height to increase if area is to be conserved.

Application to Mass Spectrometer Data

Mass spectrometer data are usually presented in the form of mass peaks, that is, the intensity of the ion current plotted versus mass. The peak height, or more generally the area under the peak, is proportional to the relative abundance of that mass. If there is any overlap, peak location and area or height will be correspondingly in error. Therefore it is desirable to unfold the overlapping peaks to obtain enhanced resolution for better quantification.

The choice of the response function will affect the resulting deconvolved data. In mass spectrometry, even if the exit slit of the spectrometer is made infinitesimally narrow, there will be a finite intrinsic width of the resulting mass peaks because of other effects, e.g., the intrinsic spatial distribution of the ions. The response function for the deconvolution is sometimes chosen as a Guassian for mass spectrometer data. A better function, however, is one obtained for the particular instrument. The response function describing the instrumental and other broadening factors in the experiment can be determined by using an isolated mass peak near those being deconvolved if the input is assumed to be

a delta function. The response function may be approximately a Gaussian curve but in general it is not.

The data treated were obtained from a five-inch radius Dempster magnetic deflection mass spectrometer (CEC 21-104). The resolution of the instrument was adjusted by varying the exit slit width. The highest resolution used was about one part in 2500.

The data shown in the figures (except for the response functions) are for mass spectrometer scans across mass 16. An isolated mass peak for argon, mass 19.9826, was used to deduce the response function. The first set of figures (Figs. 1-5) is based on data obtained from a mixture of oxygen (mass 15.9949) and methane (mass 16.0312) taken at two intermediate exit slit widths, one narrower than the other but neither having high enough resolution to separate the two peaks. The oxygen abundance was much smaller than that of the methane, producing a difficult case for deconvolution. The absence of high frequencies in the response function of the instrument limits the amount of high frequency restoration possible in deconvolution, especially without the application of constraints. The missing high frequencies can produce Gibbs oscillations, also called sidelobes or spurious oscillations. The Gibbs oscillations about the baseline of a large mass peak can easily

overwhelm a neighboring small peak. Low-pass inverse filtering is not in general capable of deconvolving to resolve the smaller peak.

In Fig. 1, curves A and B are the wider slit and narrower slit original data, respectively, while curves C and D are the wide and narrow slit argon peaks, used as response functions. The mass scale in Fig. 1 was chosen to give an expanded view of the original data. The ordinate is an arbitrary intensity scale. New abscissas and ordinate scales are needed for Figs. 2 through 4 to show the deconvolved results. The same scales are used for all three figures. Fig. 2A is the original wider slit peak (Fig. 1A) drawn to the new scales. The low-pass inverse-filtered result is in Fig. 2B. Although the first positive side lobe on the left of the methane peak is larger than the corresponding lobe on the right, one would be hard pressed to identify the oxygen peak. The function-continuation-Fourier method, Fig. 2C, offers considerable improvement. There remains enough side lobe effect, however, to make interpretation of the oxygen peak difficult. Fig. 2D gives the iterative result of 30 noise removal iterations and 150 deconvolution iterations. The Gibbs oscillations have been suppressed and the oxygen peak can be quantified with some confidence.

Fig. 3 presents a similar set of operations on the narrower slit data. The original data are curve A. The low-pass inverse-filtered result (curve B) is again dominated around the baseline

by the Gibbs oscillations. The function-continuation-Fourier result (curve C) gives marked improvement,while the result of 30 noise removal iterations and 100 deconvolution iterations (curve D) allows accurate determination of the peak height and area for the oxygen peak.

In Fig. 4, the iterative deconvolution results for the wider and narrower slit widths (curves C and D) are compared to show that the two agree. The original data are shown in curves A and B. The difference in intensity of the two results is reflective of the decreased signal available with a narrower slit width. An interesting lesson is that the choice of the highest available instrumental resolution does not necessarily lead to the optimum deconvolved result.

In iterative deconvolution the sidelobes are surpressed gradually as the constraints are applied at each iteration. Eliminating the negative lobe causes the corresponding positive lobe to be reduced also. If, as in our case, the large peak sidelobes are comparable in size to an adjacent small data peak,the latter can be seriously affected by the lobes superimposed on it. In the early iterations, before the constraints have had sufficient effect, the deconvolved result may therefore be misleading. This is illustrated by Fig. 5. New ordinate and abscissa scales have been selected for clarity. The original narrower slit data is given by curve A. Curves B, C, and D are the results of 30 noise removal iterations and 10, 20, and 100 iterations of deconvolution,respectively.

After ten iterations a peak appears at an incorrect location. At twenty iterations the indication is that small amounts of two masses are present, neither at the correct oxygen location. Finally, as the iterations converge, the constraints have their full effect and the oxygen peak is revealed correctly, in agreement with the wider slit data.

The second set of data, Figs. 6 through 9 (all drawn with the same ordinate and abscissa scales), also show a mixture of oxygen and methane. For this case, however, the higher resolution slit width was narrow enough to resolve the two peaks. The narrower slit data were therefore not deconvolved, although they could have been had more sharply defined data been needed. Rather they were used to check the correctness of the deconvolution of the low resolution result. For this experiment the oxygen and methane abundances were more nearly the same than the abundances in the previous case, so that neither peak is as seriously affected by the Gibbs oscillations of the other after deconvolution as the oxygen peak in Figs. 2 and 3.

In Fig. 6A the wide slit oxygen-methane data are shown and in Fig. 6B the argon data, resolved with the same exit slit width to reveal the instrument response. Because this response is so broad compared to the separation of the two peaks, it is difficult to determine from an examination of curve A just how many species are present and in what abundances.

The original data are repeated in Fig. 7A for comparison.

Fig. 7B is the result of 30 noise removal and 50 deconvolution iterations. It may be compared to Fig. 7C which is the narrow slit data. The deconvolution has correctly disclosed the locations and areas of the two peaks.

A small peak has also appeared to the right of the methane in Fig. 7B, at mass number 16.0605. We suggest three possibilities for this peak. The first is that it is an uncancelled positive Gibbs oscillation. The second is that it is due to the formation of a metastable ion by decomposition in the field-free drift region of the mass spectrometer. The third suggestion is that it is due to a long, slow-decay tail on the high mass side of the oxygen peak that characterized all the oxygen peaks and none of the other mass peaks observed in our work. As yet, the cause of this tail is unknown, although it may be due to an oxygen-surface interaction in the electron multiplier. If the oxygen tail can be modelled as a convolution with the other instrumental broadening factors, then deconvolution would not produce a spurious peak from the tail effect, only a skewness in the deconvolved oxygen peak. If the tail cannot be described by a convolution model, however, then the effect of deconvolution is not easily predictable. Work is continuing to discover the cause of the oxygen tail and to characterize it and also to determine whether metastable ions are formed.

The fourth and still smaller peak on the right in curve B

of Fig. 7 is almost certainly an uncancelled positive Gibbs oscillation. Such lack of cancelling can occur when the Gibbs oscillations of two large adjacent peaks interfere with each other and the amounts of positive and negative areas in the lobes are no longer nearly equal. That this is the likely interpretation for this peak can be seen in the next two figures. As both these small peaks show, the results of deconvolution must be examined carefully for effects due to the absence of high frequencies. In addition, if steps are not taken to reduce the noise sufficiently, then the noise amplification which generally occurs with deconvolution can also add spurious oscillations.

Fig. 8 consists of the original data (curve A), the result of low-pass inverse filtering (curve B), the function-continuation Fourier result (curve C), and the narrow slit data (curve D). Both deconvolution methods correctly delineate the two main peaks. Both also include significant sidelobes although these are reduced somewhat by the function-continuation method.

A comparison of the iterative (curve A) and the function-continuation Fourier (curve B) deconvolutions are contained in Fig. 9. The two approaches show good agreement for the main peaks. The juxtaposition also reveals that the small peaks of the iterative result may well both be remnants of what are probably Gibbs oscillations exhibited in curve B. This case illustrates the usefulness of employing more than one approach to deconvolution to aid in identifying features correctly.

REFERENCES

Bracewell, R. N. and Roberts, J. A., 1954, Aerial smoothing in radio astronomy: Australian J. Phys., v. 7, p. 615-640.

Bracewell, R. N., 1965, The Fourier transform and its applications: New York, McGraw-Hill; 1978, 2nd edition.

Brigham, E. O., 1974, The fast Fourier transform: New Jersey, Prentice-Hall.

van Cittert, P. H., 1931, Zum Einfluss der Spaltbreite auf die Intensitatsverteilung in Spektrallinien: Z. Physik., v. 69, p. 298-308.

Frieden, B. R., 1975, Image enhancement and restoration, in T. S. Huang, ed., Picture processing and digital filtering: Berlin, Springer-Verlag, p. 177-248; 1979, 2nd updated edition.

Frieden, B. R., 1979, private communication.

Harris, F. J., 1978, On the use of windows for harmonic analysis with the discrete Fourier transform: Proc. IEEE, v. 66, p. 51-84.

Hill, N. R., 1973, Deconvolution for resolution enhancement: M.S. thesis, University of New Orleans.

Hill, N. R. and Ioup, G. E., 1976, Convergence of the van Cittert iterative method of deconvolution: J. Opt. Soc. Am., v. 66, p. 487-489.

Howard, S. J., 1981, Method for continuing Fourier spectra given by the fast Fourier transform: J. Opt. Soc. Am., v. 71, p. 95-98; Continuation of discrete Fourier spectra

using a minimum-negativity constraint: J. Opt. Soc. Am., v. 71, p. 819-824.

Ioup, G. E. and Thomas, B. S., 1967, Smoothing and unfolding the data of beam collision experiments: J. Chem. Phys., v. 46, p. 3959-3961.

Ioup, G. E., 1968, Analysis of low energy atomic and molecular collisions: semi-classical elastic scattering calculations and deconvolution of data: Ph.D dissertation, University of Florida.

Ioup, J. W. and Ioup, G. E., 1981, Optimum use of Morrison's iterative noise removal method prior to linear deconvolution: Bull. Am. Phys. Soc., v. 26, p. 1213.

Janssen, P. A., 1970, Method for determining the response function of a high-resolution infrared spectrometer: J. Opt. Soc. Am., v. 60, p. 184-191.

Kawata, S. and Ichioka, Y., 1980, Iterative image restoration for linearly degraded images. I. Basis: J. Opt. Soc. Am., v. 70, p. 762-768; II. Reblurring procedure: J. Opt. Soc. Am., v. 70, p. 768-772.

LaCoste, L. J. B., 1982, Deconvolution by successive approximations: Geophysics, v. 47, p. 1724-1730.

Levy, S. and Fullagar, P. K., 1981, Reconstruction of a sparse spike train from a portion of its spectrum and application to high-resolution deconvolution: Geophysics, v. 46, p. 1235-1243.

Morrison, J. D., 1963, On the optimum use of ionization efficiency data: J. Chem. Phys., v. 39, p. 200-207.

Nussbaumer, H. J., 1982, Fast Fourier transform and convolution

algorithms: Berlin, Springer-Verlag.

Oppenheim, A. V. and Schafer, R. W., 1975, Digital signal processing: New Jersey, Prentice-Hall.

Robinson, E. A. and Treitel, S., 1967, Principles of digital Wiener filtering: Geophys. Prospecting, v. 15, p. 311-333.

Vogt, J. and Pascual, C., 1972, Inverse convolution applied to the evaluation of electron impact ionization efficiency curves: Int. J. Mass Spectrom. Ion Phys., v. 9, p. 441-448.

Whitehorn, M. A., 1981, Always-convergent iterative noise removal and deconvolution for image data: M.S. thesis, University of New Orleans.

Whitehorn, M. A. and Ioup, G. E., 1981, Always-convergent iterative noise removal and deconvolution for two-dimensional images: Bull. Am. Phys. Soc., v. 26, p. 1213.

Wood, G. M., Rayborn, G. H., Ioup, J. W., Ioup, G. E., Upchurch, B. T., and Howard, S. J., 1981, Data enhancement and analysis through mathematical deconvolution of signals from scientific measuring instruments: International congress on instrumentation in aerospace simulation facilities '81 Record, p. 25-37.

Wright, K. A. R, 1980, A study of Morrison's iterative noise removal method: M.S. thesis, University of New Orleans.

Wright, K. A. R. and Ioup, G. E., 1981, Optimum use of Morrison's iterative noise removal method for noise minimization: Bull. Am. Phys. Soc., v. 26, p. 1213.

Yoerger, E. J., 1978, Application of iterative smoothing and deconvolution to two-dimensional images: M.S. thesis, University of New Orleans.

W.C.Bivens, Resolution Enhancement for Non-Fixed Linear Systems, Master's Thesis, Univ. of New Orleans, 1976

H.C. Andrews, Two-Dimensional Transforms, in T.S.Huang, ed., Picture Processing and Digital Filtering, Vol. 6, Topics in Applied Physics, Springer-Verlag, Berlin, 1975

G. DiCola, A. Rota, and G. Bertolini, IEEE Trans. Nucl. Sci. NS-14, 640 (1967)

S. G. Rautian, Sov. Phys.-Usp. 66, 245 (1958)

P.E. Siska, J. Chem. Phys. 59, 6052 (1973)

J. E. Houston and R. L. Park, Rev. Sci. Instr. 43, 2437 (1972)

D. C. Morton and G. H. Rayborn, J. Chem. Phys. 70, 2450 (1979)

M. L. Uhrich, IEEE Trans. on Audio and Electroacoustics, 170 (1969)

G. D. Bergland, IEEE Spectrum, 41 (1969)

J. W. Cooley and J. W. Tukey, Math. of Compt. 19, 297 (1965)

S. J. Howard, New Techniques in Fourier Deconvolution of Gas Chromatographic Data, Master's Thesis, Univ. of Southern Miss., 1978

R. L. Field, The Gibbs Phenomenon and Resolution Enhancement, Master's Thesis, Univ. of New Orleans, 1976

A. J. Zeringue, The Gibbs Phenomenon for Gaussian, Lorentzian, and Triangle Functions, Master's Thesis, Univ. of New Orleans, 1977

A. Mendez Amaya, W. L. Mead, A. G. Brenton, C. J. Proctor, and J. H. Beynon, Int. J. Mass Spec. and Ion Phys. 36, 57 (1980)

FIGURE CAPTIONS

Figure 1. First case original oxygen-methane data at mass 16 for two exit slit widths and argon data at mass 20 and the same slit widths for instrument response determination: A) wider slit, mass 16 data, B) narrower slit, mass 16 data, C) argon wider slit data, and D) argon narrower slit data.

Figure 2. First case original and deconvolved wider slit width data: A) original data, B) after low-pass inverse-filter, C) after function-continuation Fourier deconvolution, and D) after 30 noise removal and 150 deconvolution iterations.

Figure 3. First case original and deconvolved narrower slit width data: A) original data, B) after low-pass inverse-filter, C) after function-continuation Fourier deconvolution, and D) after 30 noise removal and 100 deconvolution iterations.

Figure 4. First case original and iteratively deconvolved wider and narrower slit data: A) wider slit original data, B) narrower slit original data, C) wider slit data after 30 noise removal and 150 deconvolution iterations, and D) narrower slit data after 30 noise removal and 100 deconvolution iterations.

Figure 5. First case narrower slit data, original and different numbers of deconvolution iterations, to show constraints

gradually suppressing the effects of Gibbs oscillations: A) original data; 30 noise removal and B) 10, C) 20, and D) 100 noise removal iterations.

Figure 6. Second case: A) original wide slit oxygen-methane data and B) original argon data for response determination.

Figure 7. Second case: A) original and B) iteratively deconvolved (30 noise removal and 50 deconvolution iterations) wide slit data; C) original narrow slit data.

Figure 8. Second case: A) original, B) low-pass inverse filtered, and C) function-continuation Fourier deconvolved wide slit data; C) original narrow slit data.

Figure 9. Two different deconvolutions of the second case original wide slit data to show that the extra peaks in the iterative deconvolution could be due to uncancelled positive lobes of Gibbs oscillations: A) result of 30 noise removal and 50 deconvolution iterations and B) result of function-continuation Fourier deconvolution.

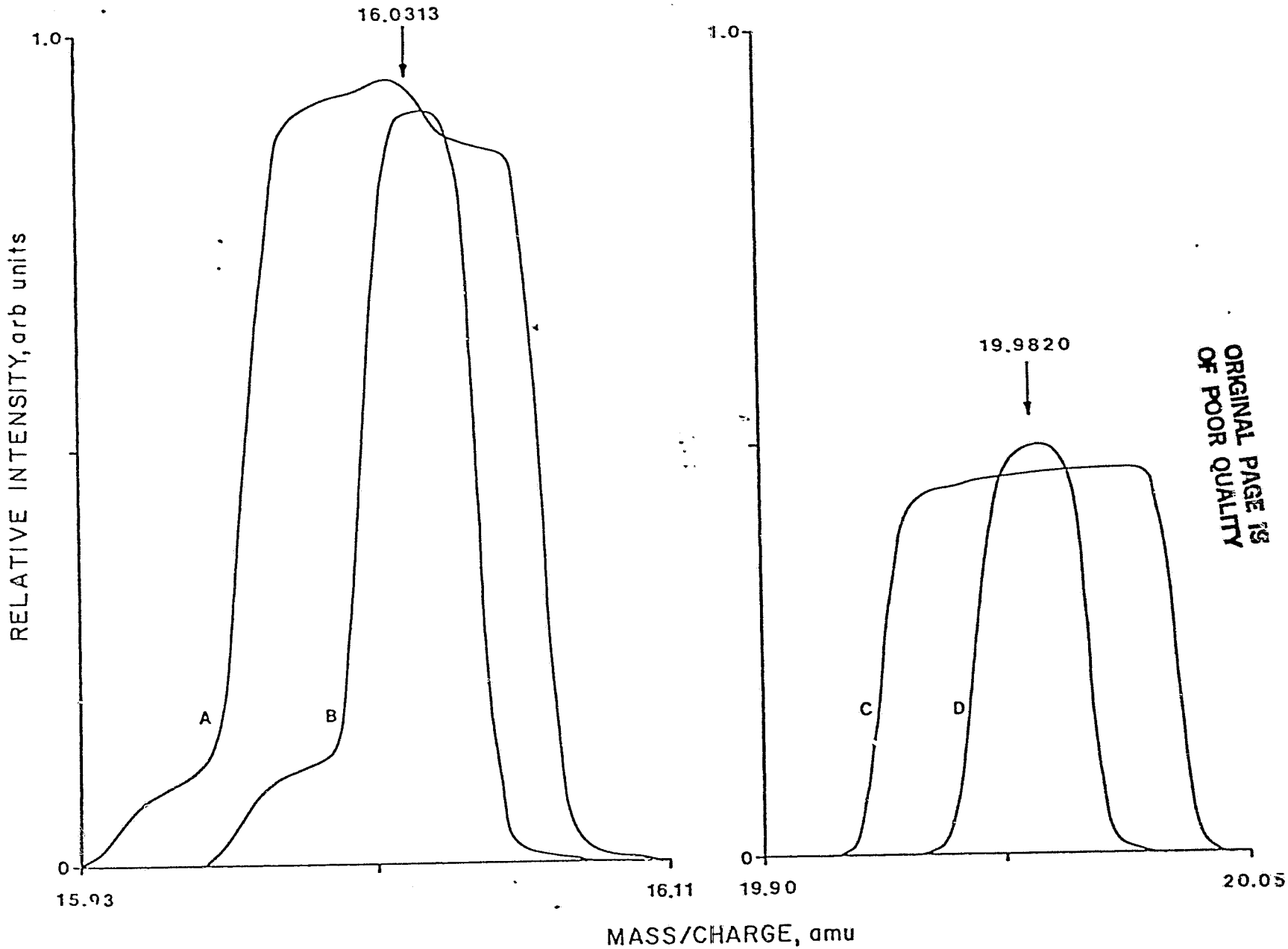

Fig. 1

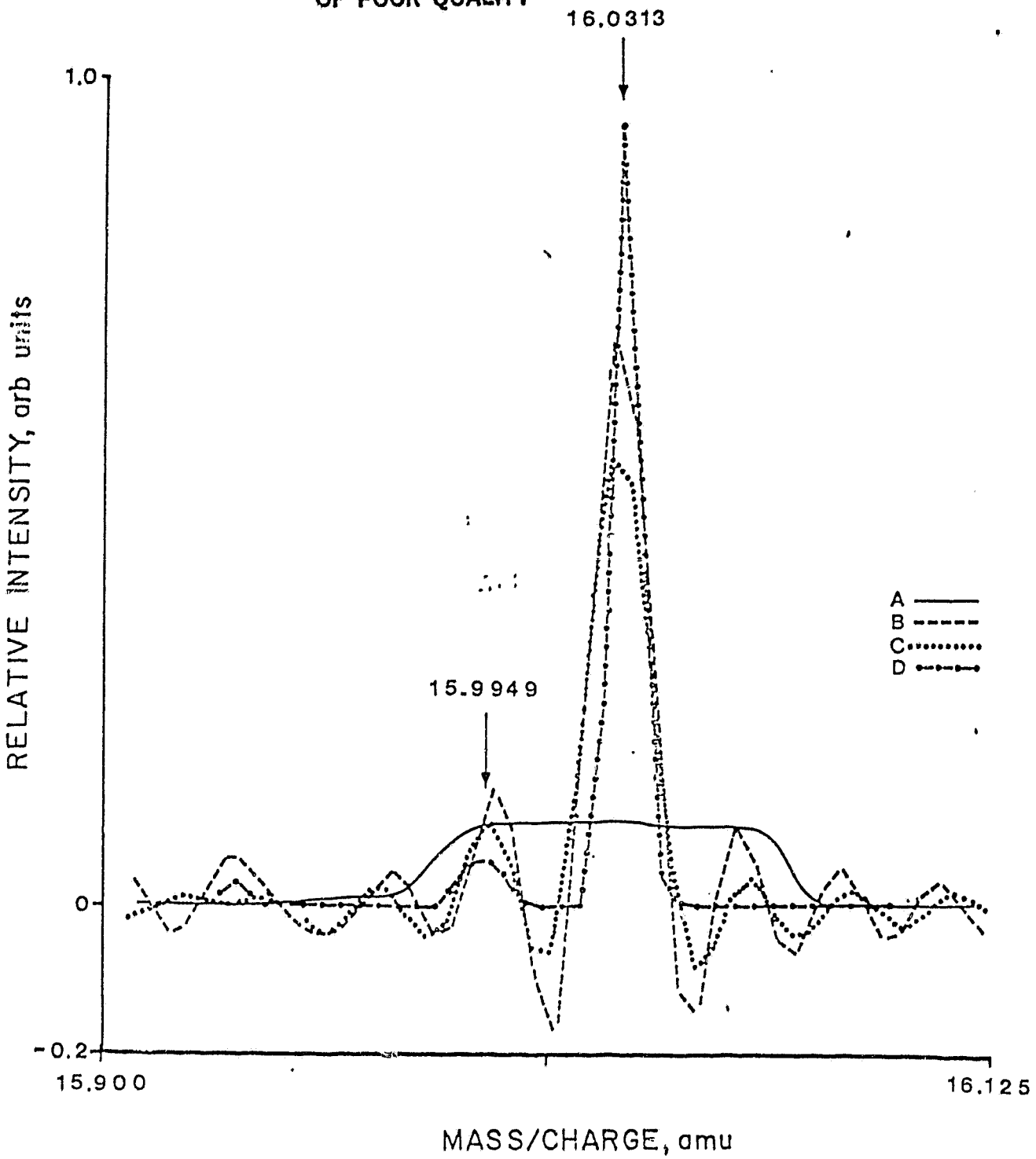

Fig. 2

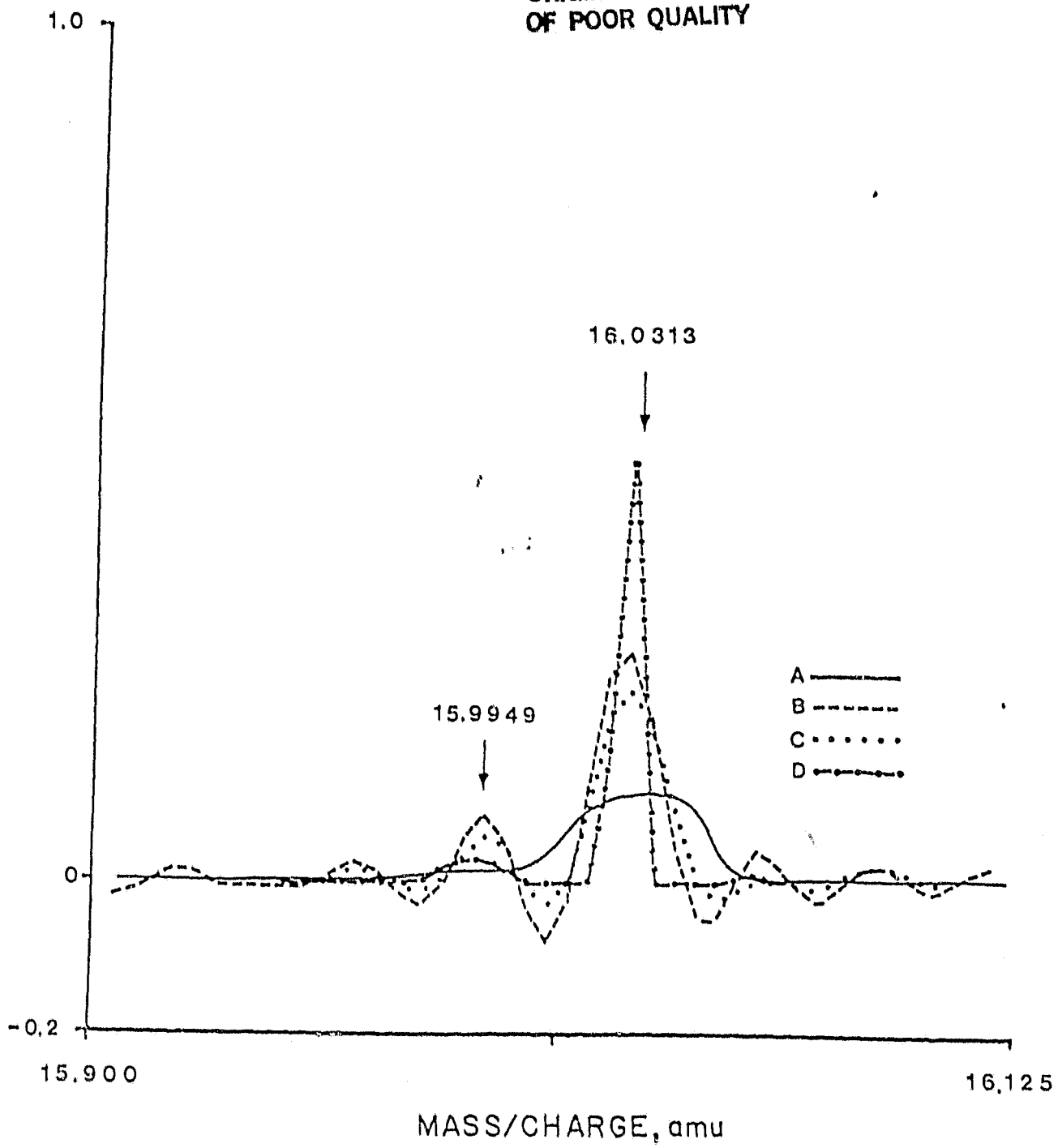

Fig. 3

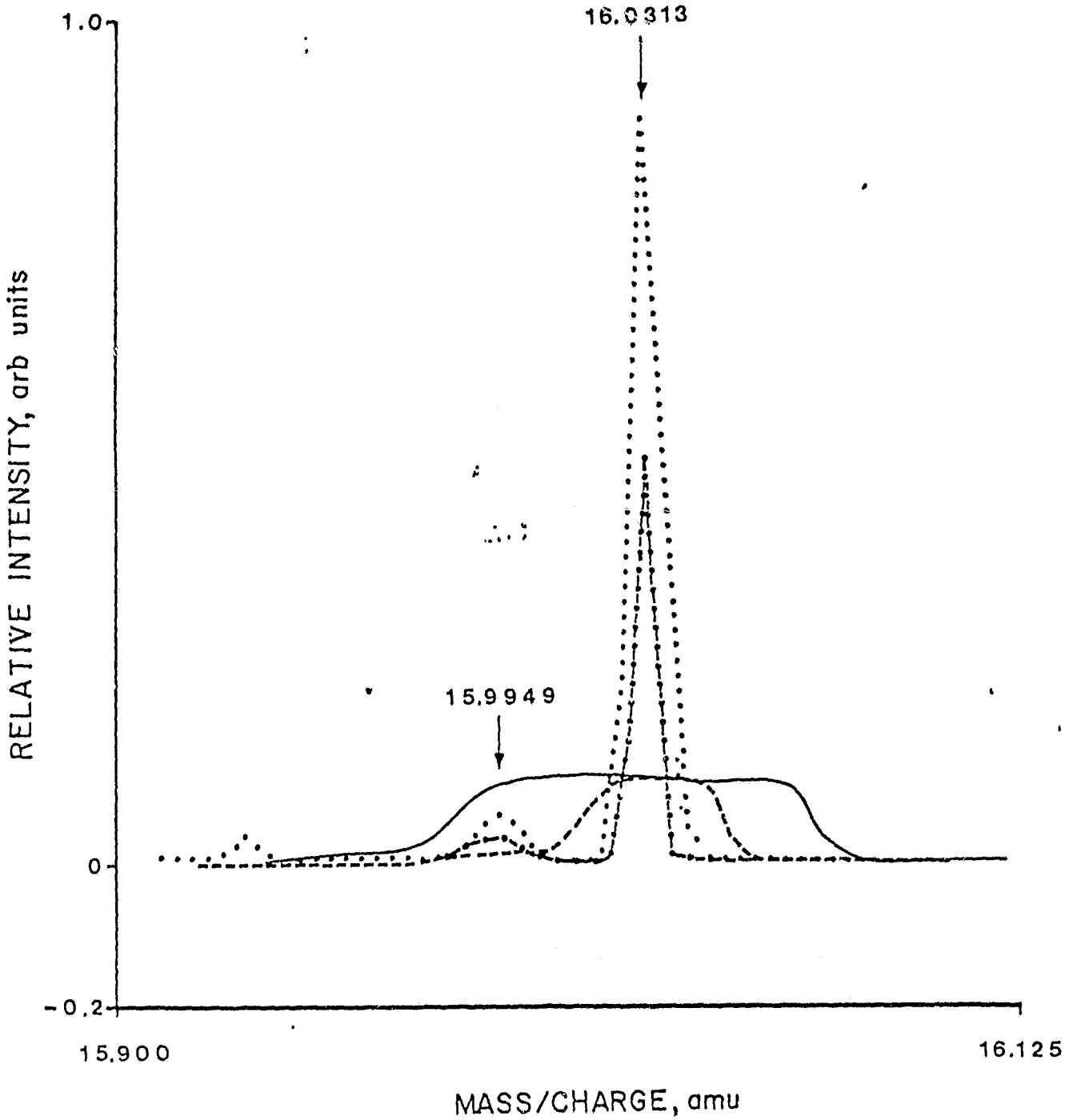

Fig. 4

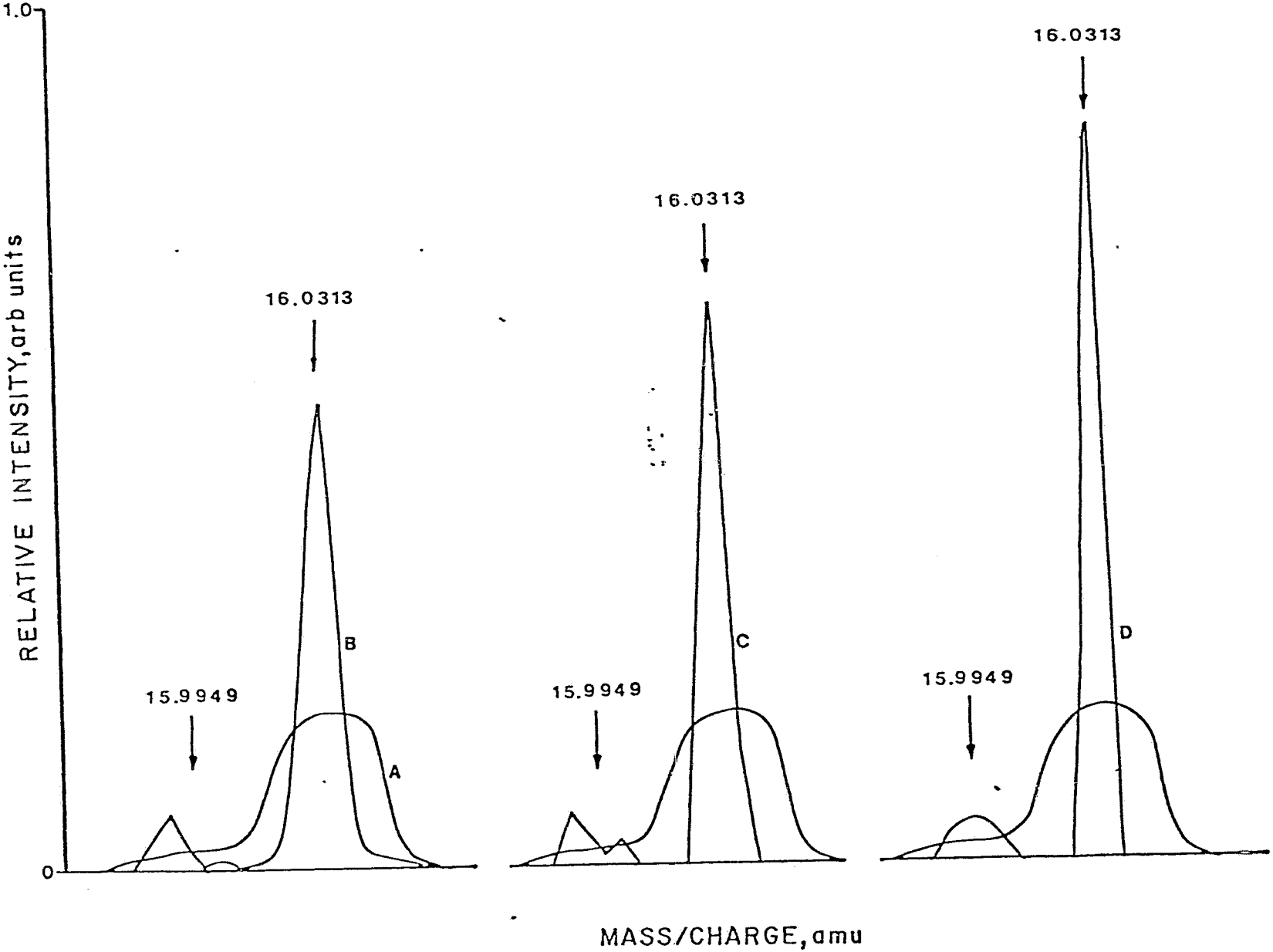
1.0
0
RELATIVE INTENSITY, arb units
16.0313
16.0313
16.0313
15.9949
15.9949
15.9949
A
B
C
D
MASS/CHARGE, amu

Fig, 5

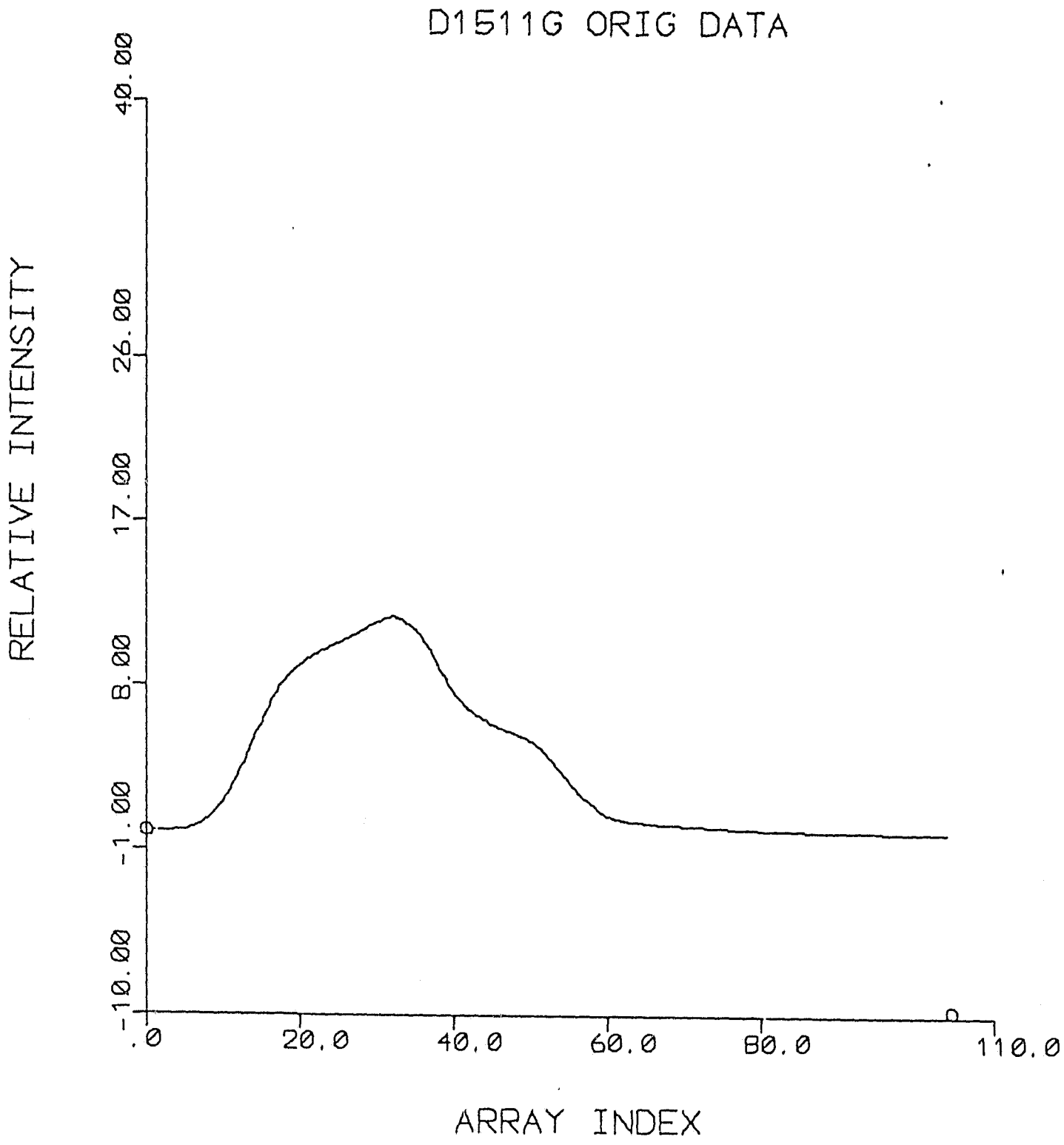

Fig. 6A, 7A, and 8A

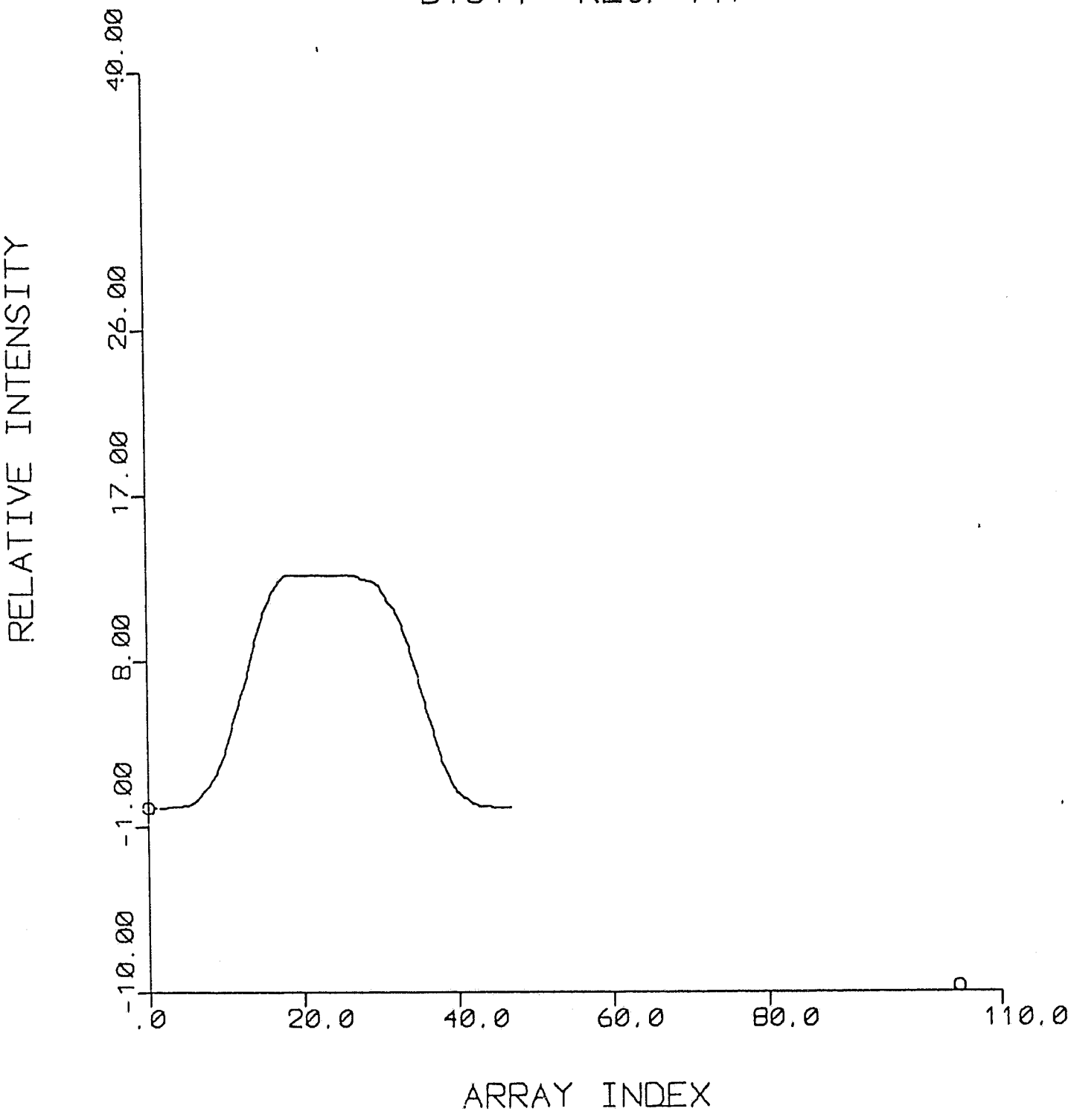

Fig. 6B

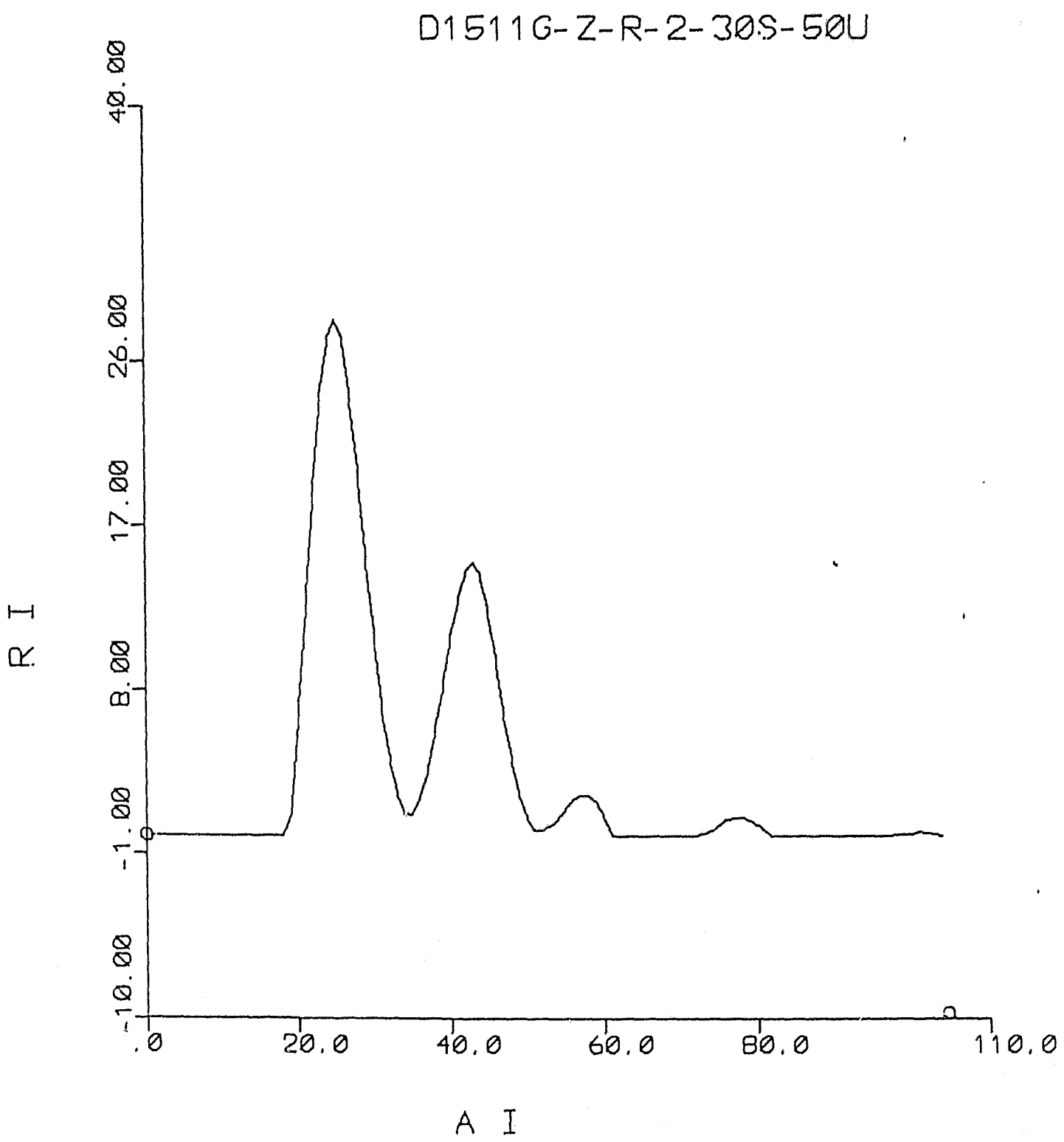

Fig. 7B and 9A

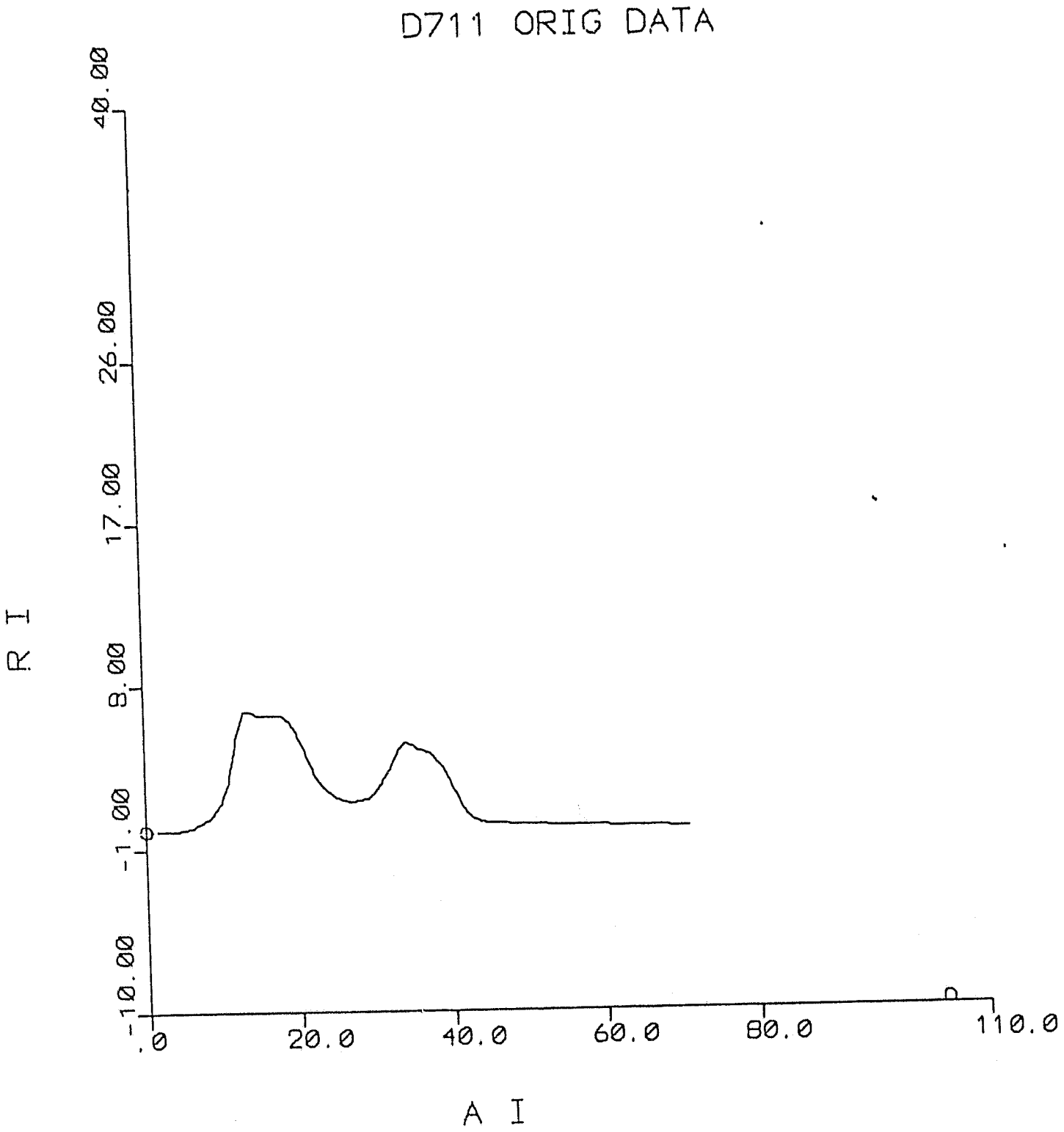

Fig. 7C and 8D

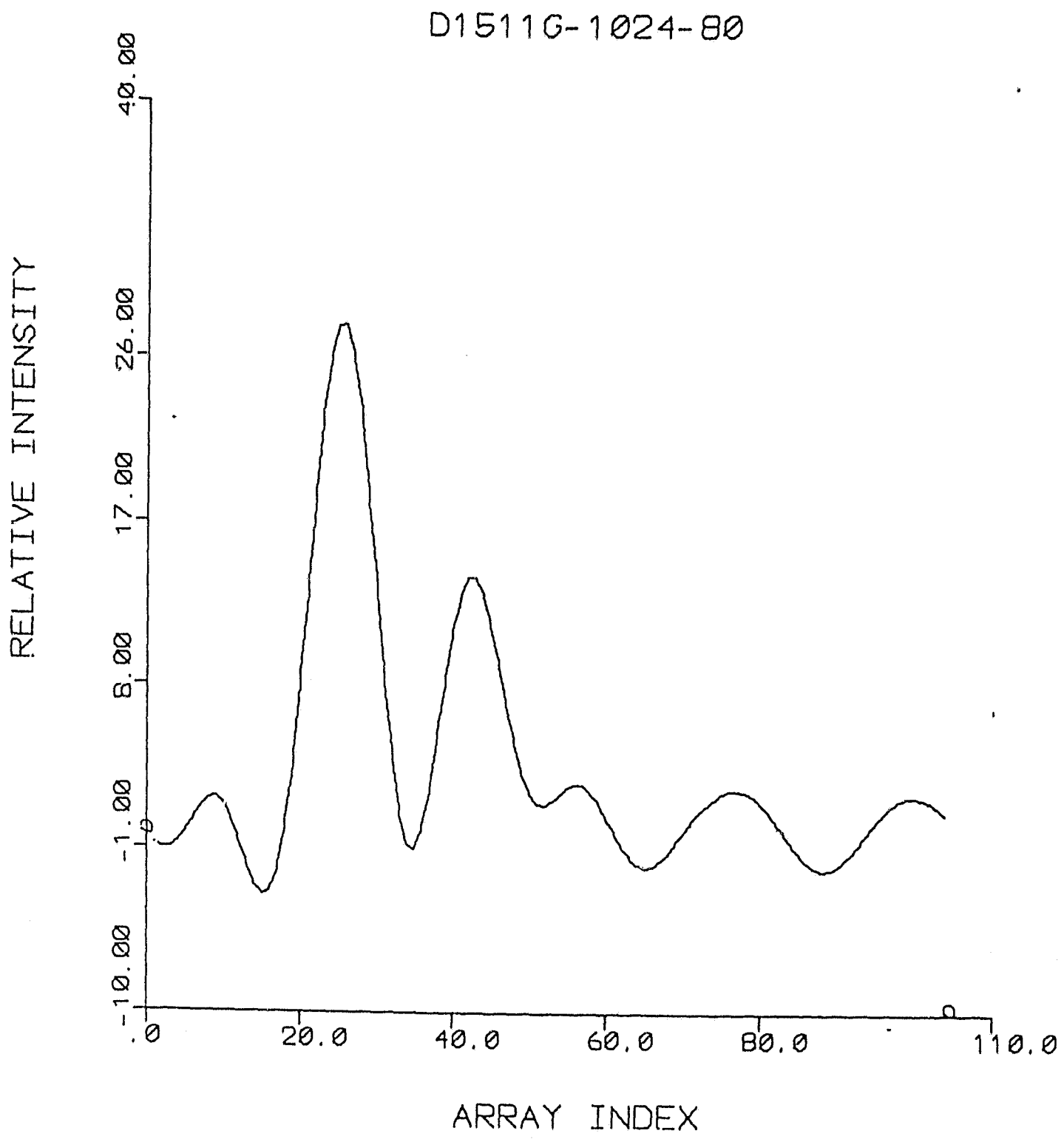

Fig. 8B

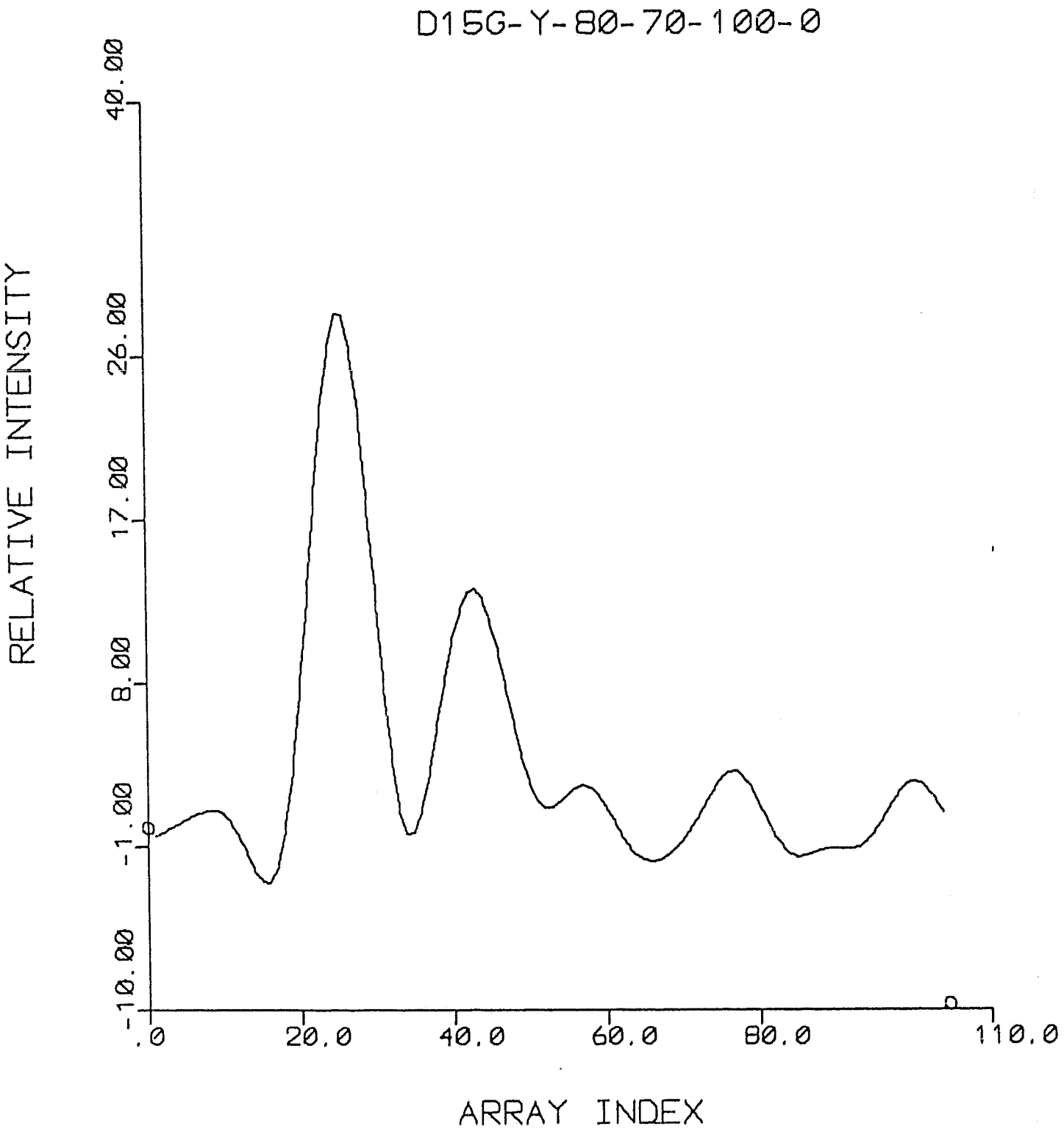

Fig. 8C and 9B